SPRAY, IGNITION, AND COMBUSTION MODELING OF BIODIESEL FUELS FOR INVESTIGATING NO_X EMISSIONS

W. Yuan, A. C. Hansen, M. E. Tat, J. H. Van Gerpen, Z. Tan

ABSTRACT. *The objective of this research was to develop a detailed numerical spray atomization, ignition, and combustion model for direct-injection diesel engines using KIVA3V code that could be applied to biodiesel fuels for investigating NO_x emissions. Several modified or recalibrated submodels were incorporated into KIVA3V, including a KH-RT spray breakup model, a Shell ignition model, and a single-step kinetic combustion model. This modified model was applied to a John Deere 4045T direct-injection diesel engine fueled by a soybean methyl ester, a yellow grease methyl ester, and No. 2 diesel fuel. The output of the model was in close agreement with the experimental measurements of cylinder pressure and heat release rate from this engine. It was predicted from the modeling results that the two biodiesel fuels had shorter ignition delay and higher overall cylinder temperatures than diesel fuel. The in-cylinder spray analysis indicated that the soybean methyl ester had slightly longer penetration than diesel fuel, but the yellow grease methyl ester had shorter penetration than diesel fuel. Fewer particle numbers were predicted for the two biodiesel fuels. Both soybean methyl ester and yellow grease methyl ester had more widespread high-temperature distribution areas than diesel fuel, which could account for the increases in NO_x emissions typically measured for biodiesel fuels.*

Keywords. *Biodiesel, Combustion, Ignition, Modeling, NO_x, Spray.*

Agricultural fats and oils, in raw or chemically modified forms, have the potential to supplant a fraction of petroleum-based fuels. Biodiesel is of particular interest to the automobile industry because it significantly reduces particulate matter (PM), hydrocarbon (HC), and carbon monoxide (CO) emissions and the net production of carbon dioxide (CO_2) from combustion sources, while no modifications are necessary to the engines. Biodiesel is also the only alternative fuel that has passed the EPA-required Tier I and Tier II Health Effects testing requirements of the Clean Air Act Amendments of 1990. In addition, biodiesel is particularly attractive because it is a renewable fuel that can be replenished through the growth of plants or production of livestock, and it has the potential to supplant a fraction of petroleum-based fuels.

Many researchers have found that although biodiesel fuels could reduce PM, CO, and HC exhaust emissions, NO_x emissions were increased compared to petroleum-based diesel fuel in diesel engines (Sharp et al., 2000; McCormick et al., 2001; Grimaldi et al., 2002; Tat and Van Gerpen, 2003). Most of these researchers focused only on experimental studies. The fundamental principles of the NO_x increase are still unclear. This has motivated interest in modeling the spray, ignition, and combustion of biodiesel. The objective of this work was to develop a detailed numerical spray atomization, ignition, and combustion model for direct-injection diesel engines using KIVA3V code that could be applied to biodiesel fuels. The ultimate goal of this research is to use this model to investigate the NO_x emissions mechanism of biodiesel and diesel fuel.

This article reports on efforts to use the engine simulation program KIVA-3V (Amsden, 1997) to characterize the ignition, spray, and combustion of the soybean oil and yellow grease based biodiesel fuels and No. 2 diesel in a DI diesel engine. The simulation models are briefly introduced, and the fuel properties and engine specifications are presented. The simulation output of the three fuels is compared.

Article was submitted for review in November 2004; approved for publication by Power & Machinery Division of ASAE in April 2005. Presented at the 2004 ASAE Annual Meeting as Paper No. 046087.

The authors are **Wenqiao Yuan, ASAE Student Member,** PhD Student, and **Alan C. Hansen, ASAE Member Engineer,** Associate Professor, Department of Agricultural and Biological Engineering, University of Illinois at Urbana-Champaign, Urbana, Illinois; **Mustafa E. Tat,** Assistant Professor, Department of Mechanical Engineering, Osmangazi University, Turkey; **Jon H. Van Gerpen, ASAE Member Engineer,** Professor, Department of Biological and Agricultural Engineering, University of Idaho, Moscow, Idaho; and **Zhongchao Tan, ASAE Member Engineer,** Assistant Professor, Department of Mechanical Engineering, University of Calgary, Alberta, Canada. **Corresponding author:** Alan C. Hansen, 360 AESB, 1304 W. Pennsylvania Avenue, Urbana, IL 61801; phone: 217-333-2969; fax: 217-244-0323; e-mail: achansen@uiuc.edu.

COMPUTATIONAL MODELS

KIVA-3V is a fully three-dimensional fluid dynamics model for chemically reacting flows (Amsden, 1997). Its submodels were originally developed for petroleum-based fuels, such as gasoline and diesel. There are very few published applications of the KIVA program involving biodiesel. This section presents the models that were modified or added to KIVA-3V to include biodiesel in the fuel library.

SPRAY BREAKUP MODEL

The Kelvin-Helmholtz Rayleigh-Taylor (KH-RT) model (Ricart et al., 1997) was used to represent spray breakup in this study. The basis of this model was the concept introduced

by Reitz and Diwakar (1987) that the atomization of the injected liquid and the subsequent breakup of drops were indistinguishable processes within a dense spray. The liquid injection was simulated using the "blob" injection method (Reitz and Diwakar, 1987), and the wave model (Reid, 1987) was employed to describe the droplet breakup due to shear flow.

The radius (r) of the new droplets from the breakup of a parent droplet or blob is described as follows (Ricart et al. 1997):

$$r_c = B_0 \Lambda \tag{1}$$

where $B_0 = 0.61$, which is a constant built into the code, and Λ is the wavelength corresponding to the fastest growing K-H wave frequency (Ω), which is given by:

$$\Omega = \frac{0.34 + 0.38We^{1.5}}{(1+Z)(1.4T^{0.6})}\sqrt{\frac{\sigma}{\rho_l r^3}} \tag{2}$$

$$\Lambda = \frac{9.02r(1+0.45\sqrt{Z})(1+0.4T^{0.7})}{(1+0.865We^{1.67})^{0.6}} \tag{3}$$

where

$We = \frac{\rho_g u_r^2 r}{\sigma}$ = gas Weber number

$Z = \frac{\sqrt{We_l}}{\mathrm{Re}_l}$ = Ohnesorge number

$We_l = \frac{\rho_l u_r^2 r}{\sigma}$ = liquid Weber number

$\mathrm{Re}_l = \frac{u_r r \rho_l}{\mu_l}$ = liquid Reynolds number

$T = Z\sqrt{We}$ = Taylor number

and u_r is the relative velocity, σ is the surface tension, μ_l is the liquid viscosity of the droplets, and ρ_λ and ρ_γ are the droplet and gas density, respectively.

The change of the radius (r) of the parent droplet due to breakup is:

$$\frac{dr}{dt} = \frac{r - r_c}{\tau_b} \tag{4}$$

where $\tau_b = \frac{3.788B_1 r}{\Omega\Lambda}$, which is the characteristic K-H wave breakup time, and $B_1 = 1.0$, which is a constant built into the code.

In addition to the K-H type instability, Ricart et al. (1997) suggested that the Rayleigh-Taylor (RT) instability might also play an important role because the liquid droplets experience very high initial velocities and rapidly decelerate due to drag forces. Similar to the K-H wave breakup, the wavelength (Λ_{RT}) corresponding to the fastest growing R-T wave frequency (Ω_{RT}) and the wave number (K_{RT}) are formulated as (Bellman and Pennington, 1954):

$$\Lambda_{RT} = \frac{\pi B_2}{K_{RT}} \tag{5}$$

$$\Omega_{RT} = \sqrt{\frac{2\left[-g_t(\rho_l - \rho_g)\right]^{3/2}}{3\sqrt{3\sigma}(\rho_l + \rho_g)}} \tag{6}$$

$$K_{RT} = \sqrt{\frac{-g_t(\rho_l - \rho_g)}{3\sigma}} \tag{7}$$

where $B_2 = 0.1$, which is a constant built into the code; $gt = (\vec{g} + \vec{a})\vec{j}$, which is the acceleration in the direction of droplet travel; $\vec{g}$ and $\vec{a}$ are the gravity and droplet acceleration, respectively; and $\vec{j}$ is the unit vector tangential to the droplet trajectory.

The R-T wave breakup time (τ_{RT}) is represented as:

$$\tau_{RT} = \frac{B_3}{\Omega_{RT}} \tag{8}$$

where $B_3 = 1.0$, which is a constant built into the code.

The constants B_0, B_1, B_2, and B_3 were built into the code. Except for B_1, these constants were correctly calibrated in the model, so they do not need modifications. However, B_1 was found to be related to the initial disturbance level in the breakup process, and it was dependent on injector design (Kong et al., 1995). Therefore, B_1 was calibrated in the model and was determined as 1.0.

In the overall model, the K-H and R-T submodels compete to break up the droplet (Ricart et al. 1997). The R-H model compared the wavelength to the droplet radius. If the wavelength was smaller than the droplet radius, then the model assumed that the wave was growing on the surface of the droplet, and the time of the growth was tracked and compared to the breakup time. Once the time was greater than the breakup time, the R-H breakup occurred. The K-H model was activated whenever the droplet radius was bigger than the K-H wavelength.

It should be noted that the KH-RT model was developed originally for diesel engines fueled by diesel fuels. However, it is a physically based model, which means it can be extended to other fuels provided the physical properties are well defined. This is the reason why this model was selected to simulate the breakup of biodiesel fuel sprays as well as diesel fuel.

Shell Auto-Ignition Model

Among the parameters in diesel engine operation, ignition delay is considered to be critical to both the performance and the emissions of diesel engines. During the delay period, the injected fuel undergoes a series of complex processes such as atomization, collision, vaporization, and preliminary chemical reactions. Several approaches have been made to model the auto-ignition phenomena in multidimensional modeling of diesel engines with diesel fuels. Among these approaches, single-step irreversible Arrhenius kinetics models have often been utilized because it is easy to apply the models in computational fluid dynamics (CFD) codes and the results are reasonably accurate when some parameters are adjusted for different engine operating conditions. However, this model is not able to simulate the low-temperature auto-ignition process accurately in diesel engine conditions. This motivated the interest in multi-step models. The Shell model (Halstead et al., 1977) is one of the multi-step kinetics models that have been employed by many researchers. The Shell model is an eight-step chemical kinetics model. It involves some necessary generic reactions to simulate the controlling elementary reactions, i.e., initiation, propagation, branching, and termination. Successful application of the Shell model to

diesel engines can be found for the diesel fuel ignition process (Theobald and Cheng, 1987; Griend et al., 1990; Kong and Reitz, 1993; Hamosfakidis and Reitz, 2003). Eight generic reactions based on the degenerate branching characteristics of hydrocarbon auto-ignition were formulated with five generic species and were modified to account for the differences between biodiesel and diesel. The model was described in more details in a previous study (Yuan et al., 2003a).

Combustion Model

The modified Shell ignition model was combined with the single-step kinetic combustion model, which has a reaction rate given by the following equation:

$$\text{Rate} = A_{fr}[\,fuel\,]^m[O_2]^n \exp\left(\frac{-E}{RT}\right) \qquad (9)$$

where $m = 0.25$ and $n = 1.5$ for both diesel and biodiesel; A_{fr} is the forward reaction rate coefficient, which is fuel and engine dependent and needs to be adjusted to match experimental data for each fuel; and E is the activation energy of the fuel, which is set equal to 15780 kcal mol^{-1} (66068 kJ mol^{-1}) for all the test fuels. The constants in the Shell ignition model were the same for all these fuels, but A_{f1} (A_{fr} in eq. 9, where $r = 1$) in the combustion model was different for each fuel. A_{f1} has a substantial effect on combustion (Amsden, 1993). If it is too large, the KIVA combustion simulation will fail because of too high a reaction rate. If it is too small, the combustion cannot be sustained. It can only be determined empirically. Once it is defined, it will be constant for all cases in the same engine with the same fuel. A general method to predict this constant will be valuable even in the characteristic time combustion model. In this study, A_{f1} was 3.0×10^{11} and 4.5×10^{11} for diesel and biodiesel, respectively.

Model Application

Test Fuels

A soybean oil derived methyl ester (SME), a yellow grease methyl ester (YGME), and a commercial grade No. 2 diesel (D2) were tested. The selected properties of the fuels are listed in table 1. The properties of the biodiesel fuel required for combustion modeling were predicted using a computer program developed for this study (Yuan et al., 2003b, 2004). The molecular structures for D2 and the two biodiesel fuels used in the model were $C_{12}H_{26}$ and $C_{19}H_{35}O_2$, respectively. $C_{12}H_{26}$ was the recommended molecular structure for No. 2 diesel used by the Cummins model in KIVA-3V. The molecular structure of SME and YGME were defined from the fuel properties prediction model (Yuan et al., 2004).

Test Engine

A John Deere 4045T diesel engine was tested, and the experimental data of cylinder pressure, injection pressure and injector needle lift, exhaust emissions of CO, HC, NO and smoke, along with engine working condition parameters such as intake manifold temperature and pressure, and exhaust temperature were collected. The engine specifications are given in table 2. A $17 \times 12 \times 16$ mesh was used for the 90° sector of the engine cylinder, which had 13675 cells and 13871 vertices.

Table 1. Selected properties of No. 2 diesel and biodiesel fuels.

Properties	D2	SME	YGME
Carbon (% mass)	86.66	77.0	76.66
Hydrogen (% mass)	12.98	12.18	12.33
Sulfur (% mass)	0.034	<0.005	<0.005
Oxygen (% mass by difference)	--	10.82	11.01
Cetane number (ASTM D613)	42.2	50.4	62.6
Gross heat of combustion (kJ kg^{-1})	45227	39968	40128
Net heat of combustion (kJ kg^{-1})	42859	37383	37702
Kinematic viscosity @ 40°C (mm^2 s^{-1})	2.8911	4.5926	5.9156
Specific gravity	0.8559	0.8796	0.8722

Table 2. John Deere 4045T diesel engine specifications.

Bore	106.5 mm
Stroke	127.0 mm
Connecting rod length	203.0 mm
Compression ratio	17.0:1
Injector hole diameter	0.0315 cm
Injector hole number	4
Maximum power	66.5 kW at 2200 rpm
Peak torque	374 N-m at 1200 rpm

Table 3. Working conditions.

	D2	SME	YGME
Engine speed (rpm)	1400	1400	1400
Load	95%	95%	95%
Brake torque (N-m)	352.5	352.5	353.2
Intake air temperature (K)	332.1	332.6	332.1
Intake air pressure (kPa)	125.978	124.599	125.978
Start of injection (CA)	−6.4	−7.13	−7.0
End of injection (CA)	10.2	10.8	11.2
Fuel consumption rate (mg cycle^{-1})	64.426	72.739	73.177

Test Conditions

The conditions of the tested cases are listed in table 3. The same engine speed and load were applied for each fuel. Table 3 shows that the intake air temperature and pressure for each test were about the same. The increase in fuel consumption for SME and YGME is a result of their lower heat of combustion, thus requiring more fuel to maintain the same load as for D2. The variations in the start and end of injection for the three fuels were brought about by the radial piston distributor-type fuel injection system. An advance in the start of injection with increasing fuel delivery can be expected with this type of mechanical pump.

Results and Discussion

Cylinder Pressure and Heat Release Rate

Cylinder pressure and heat release rate are the most widely used indicators of modeling accuracy relative to experimental data. Figures 1 through 3 show the comparison of predicted and measured cylinder pressure and heat release rate for D2, SME, and YGME.

It can be seen from figures 1 through 3 that the predicted cylinder pressures of both diesel and biodiesel are in close agreement with their measured cylinder pressures, especially in the region of peak cylinder pressure. There are some discrepancies between predicted and measured values at about 5 crank angle degrees (° CA) before top dead center (TDC) and after 20° CA after TDC. The former discrepancy is very likely due to the absence of a blow-by model in KIVA3V, causing an overprediction of pressure. The latter

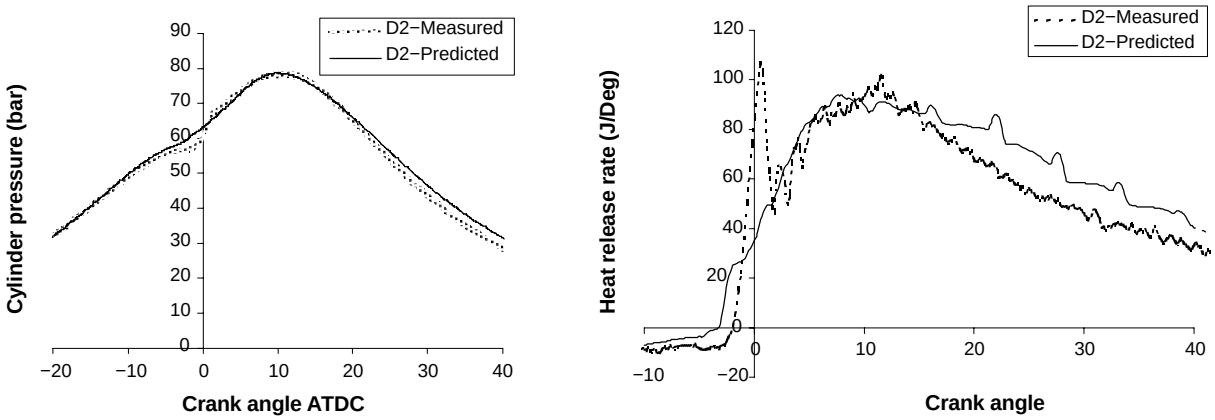

Figure 1. Measured and predicted cylinder pressures and heat release rate for D2.

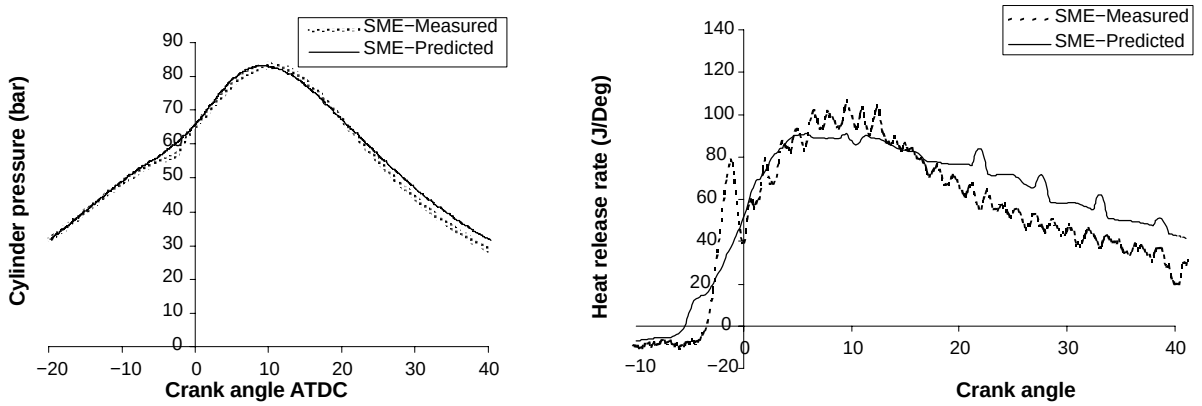

Figure 2. Measured and predicted cylinder pressures and heat release rate for SME.

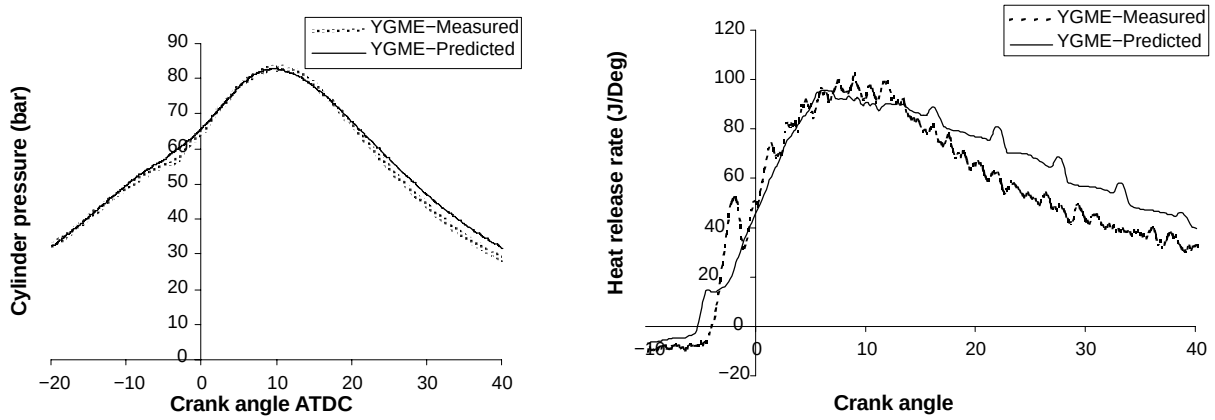

Figure 3. Measured and predicted cylinder pressures and heat release rate for YGME.

discrepancy could be attributed to an inaccurate heat loss model that underpredicted the heat loss, causing higher cylinder pressures.

The predicted heat release rates for all the tested fuels are close to the measured heat release rates, as can be seen from figures 1 through 3, especially around the peak heat release rates. However, the first peak of heat release rate from the predictions is not as prominent as from the measurements. This discrepancy is due to the overpredicted cylinder pressure at 5° CA before TDC, as mentioned earlier. Predicted start of combustion occurs earlier than the measured case, and the amount of premixed combustion, characterized by the first small peak or discontinuity in the rate of heat release curve, is much smaller in magnitude than for the rate of heat release determined from the measured cylinder pressure. This difference was attributed to the shorter ignition delay resulting in a smaller accumulation of fuel during the ignition delay period and therefore less premixed fuel and air being ready for simultaneous combustion. The difference between the measured and predicted

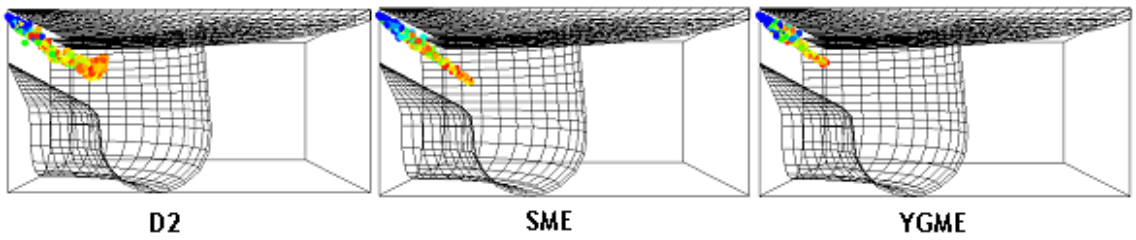

Figure 4. Longest penetrations for D2, SME, and YGME.

starts of combustion was the same for D2 and YGME at 1.25° CA but was 2.5° CA for SME. No definite reason could be found for the increase in the case of SME, although the start of injection was slightly more advanced for this fuel. The measured ignition delay, which is defined as the duration between start of injection and start of combustion was 4.6°, 3.53°, and 3.2° CA for D2, SME, and YGME, respectively. Biodiesel fuels showed shorter ignition delays than diesel fuel, and YGME had an even shorter ignition delay than SME due to a higher cetane number.

Spray Characteristics

The spray process is very important for diesel engine combustion and emissions. Spray penetration, droplet number, and particle size are key parameters for the fuel atomization and mixing process.

Penetration

A slightly increased penetration tip was predicted with SME, and shorter penetration was found for YGME compared to diesel fuel, as shown in figure 4. The slightly increased penetration tip of SME can be attributed to the smaller spray angle and bigger droplets of the SME spray, as discussed later. These results are in agreement with experimental observations of Senda et al. (2004). The shorter penetration of YGME could be due to advanced combustion of biodiesel, which caused high cylinder pressure and temperature, leading to more rapid vaporization of the fuel.

Particle Number and Size

Particle number and particle size are equivalent to the droplet number and droplet size predicted in the KH-RT spray breakup model. As shown in figure 5, fewer particle numbers for the two biodiesel fuels were predicted compared to D2. Both SME and YGME have two peaks of particle numbers. The first peak of SME occurred at −2° CA, and the first peak of YGME occurred at −2.5° CA. After the first peak, particle numbers decreased rapidly due to early combustion that caused rapid vaporization of fuel liquid droplets. Since fuel was continuously injected into the chamber, the particle numbers started to increase around TDC and reached a second peak. When combustion occurred in the overall chamber, particle numbers decreased again, and all the particles disappeared at about 10° CA. For D2, only one peak was predicted because of the retarded combustion and higher volatility of D2 compared to the biodiesel fuels. When combustion occurred, the more premixed combustion caused more rapid heat release and faster vaporization rate than with the biodiesel fuels; therefore, the continually injected fuel could not form a second peak of particle number. Considering that the amount of biodiesel fuel injected each cycle per cylinder was about 12% more than diesel in mass, the fewer particle numbers indicate bigger particle sizes of biodiesel fuels.

Combustion Analysis

The predicted in-cylinder temperature distributions of D2, SME, and YGME at crank angles of 9°, 10°, and 11° are shown in figure 6. These crank angles were selected because the peak cylinder pressure and heat release occurred at these times. It can be seen from figure 6 that the two biodiesel fuels have similar temperature distribution shapes to diesel fuel. However, the two biodiesel fuels have more widespread high-temperature distributions than D2 in the central region of the chamber cross-section. This finding was in accordance with experimental results reported by Senda et al. (2004), in which the domain temperature existed in the whole flame for

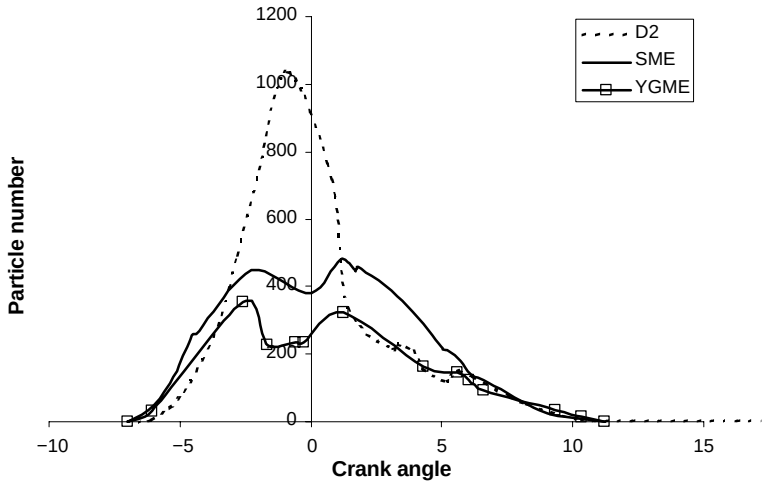

Figure 5. Sauter mean radius of diesel and biodiesel.

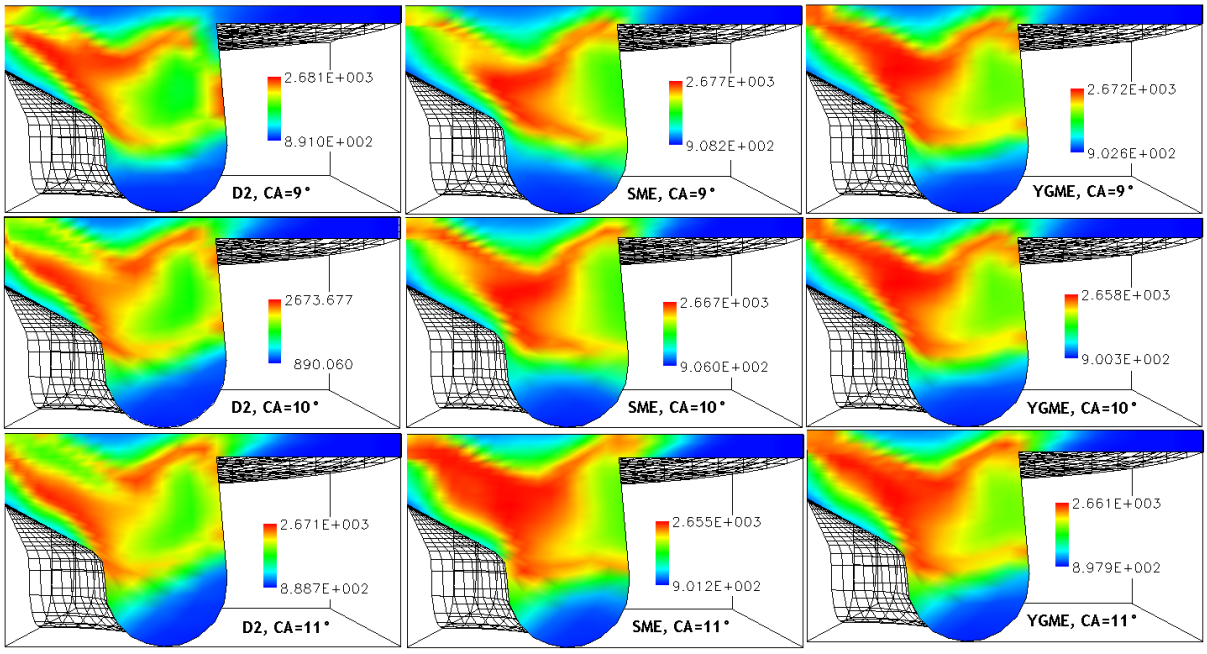

Figure 6. In-cylinder temperature distributions of D2, SME, and YGME (from left to right) at crank angles of 9˚, 10˚, and 11˚ (from top to bottom) at *y* = 0 plane.

biodiesel but only in the central part of the flame for diesel fuel. In figure 6, SME and YGME have similar temperature distributions, while SME has slightly higher temperatures than YGME.

The predicted overall cylinder temperatures are shown in figure 7. Higher cylinder temperatures were predicted for SME and YGME compared to D2. The maximum difference in temperatures was 93 K between SME and D2 and 66 K between YGME and D2 at 10˚ ATDC. This higher cylinder temperature could be a reason for higher NO_x emissions from biodiesel.

Conclusions

Several submodels have been incorporated into KIVA3V. These submodels include a KH-RT spray breakup model, a Shell ignition model, and a single-step kinetic combustion model that have been modified or calibrated for biodiesel. The modified KIVA3V model was applied to a John Deere 4045T direct-injection diesel engine fueled by a soybean methyl ester, a yellow grease methyl ester, and No. 2 diesel fuel. The output of the model was compared to and found to be in close agreement with the experimental measurements of cylinder pressure and heat release rate from this engine.

It was predicted from the modeling results that the two biodiesel fuels had shorter ignition delays and higher overall cylinder temperatures than diesel fuel. The in-cylinder spray analysis indicated that the soybean methyl ester had slightly greater penetration into the combustion chamber than diesel fuel, but the yellow grease methyl ester had shorter penetration, while fewer particle numbers were predicted for the two biodiesel fuels. Both the soybean methyl ester and yellow grease methyl ester had more widespread high-temperature distribution areas than diesel fuel, which could account for the increases in NO_x emissions typically measured for biodiesel fuels.

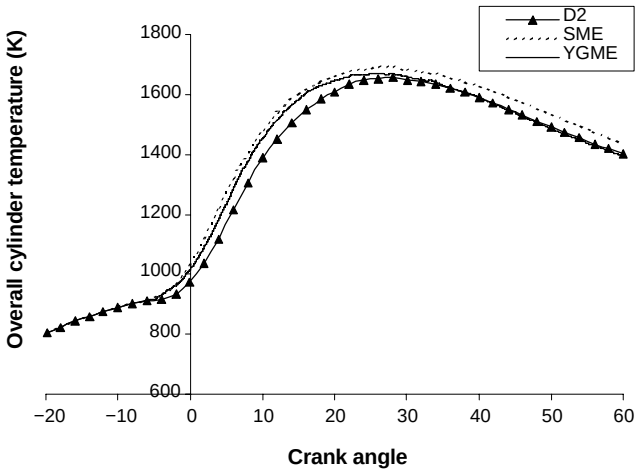

Figure 7. Overall cylinder temperatures of D2, SME, and YGME.

Acknowledgements

This material is based on work supported by the USDA Cooperative State Research, Education, and Extension Services (CSREES) under Project No. Hatch 10-311 AE. Financial support was also provided by the University of Illinois Campus Research Board.

References

Amsden, A. A. 1993. KIVA-3: A KIVA program with block-structured mesh for complex geometries. LA-12503-MS. Los Alamos, N.M.: Los Alamos National Laboratory.

Amsden, A. A. 1997. KIVA-3V: A block-structured KIVA program for engines with vertical or canted valves. LA-13313-MS. Los Alamos, N.M.: Los Alamos National Laboratory.

Bellman, R., and R. H. Pennington. 1954. Effect of surface tension and viscosity on Taylor instability. *Quarterly of Applied Math.* 12(2): 151-162.

Griend L. V., M. E. Feldman, and C. L. Peterson. 1990. Modeling combustion of alternate fuels in a DI diesel engine using KIVA. *Trans. ASAE* 33(2): 342-350.

Grimaldi, C. N., L. Postrioti, M. Battistoni, and F. Millo. 2002. Common rail HSDI diesel engine combustion and emissions with fossil/bio-derived fuel blends. SAE Tech. Paper 2002-01-6085. Warrendale, Pa.: SAE.

Halstead, M. P., L. J. Kirsch, and C. P. Quinn. 1977. The autoignition of hydrocarbon fuels at high temperatures and pressure-fitting of a mathematical model. *Combustion and Flame* 30: 45-60.

Hamosfakidis, C., and R. D. Reitz. 2003. Optimization of a hydrocarbon fuel ignition model for two single-component surrogates of diesel fuel. *Combustion and Flame* 132(3): 433-450.

Kong, S. C., and R. D. Reitz. 1993. Multidimensional modeling of diesel ignition and combustion using a multistep kinetics model. *ASME Trans., J. Eng. for Gas Turbines and Power* 115(4): 781-789,

Kong, S. C., Z. Han, and R. D. Reitz. 1995. The development and application of a diesel ignition and combustion model for multidimensional engine simulation. SAE Tech. Paper 950278. Warrendale, Pa.: SAE.

McCormick, R. L., M. S. Graboski, A. M. Herring, and T. L. Alleman. 2001. Impact of biodiesel source material and chemical structure on emissions of criteria pollutants from a heavy-duty engine. *Environ. Science and Tech.* 35(9): 1742-1747.

Reid, R. D. 1987. Modeling atomization processes in high-pressure vaporizing sprays. *Atomization and Spray Tech.* 3(4): 309-337.

Reitz, R. D., and R. Diwakar. 1987. Structure of high-pressure sprays. SAE Tech. Paper 870598. Warrendale, Pa.: SAE.

Ricart, L. M., J. Xin, G. R. Bower, and R. D. Reitz. 1997. In-cylinder measurement and modeling of liquid fuel spray penetration in a heavy-duty diesel engine. SAE Tech. Paper 971591. Warrendale, Pa.: SAE.

Senda, J., N. Okui, T. Suzuki, and H. Fujimoto. 2004. Flame structure and combustion characteristics in diesel engines fueled with biodiesel. SAE Tech. Paper 2004-01-0084. Warrendale, Pa.: SAE.

Sharp, C. A., S. A. Howell, and J. Jobe. 2000. The effect of biodiesel fuels on transient emissions from modern diesel engines: Part I. Regulated emissions and performance. SAE Tech. Paper 2000-01-1967. Warrendale, Pa.: SAE.

Tat, M., and J. H. Van Gerpen. 2003. Fuel property effects on biodiesel. ASAE Paper No. 036034. St. Joseph, Mich.: ASAE.

Theobald, M. A., and W. K. Cheng. 1987. A numerical study of diesel ignition. ASME Paper No. 87-FE-2. New York, N.Y.: ASME.

Yuan, W., A. C. Hansen, and Q. Zhang. 2003a. Computational study of biodiesel ignition in a direct-injection engine. ASAE Paper No. 036035. St. Joseph, Mich.: ASAE.

Yuan, W., A. C. Hansen, and Q. Zhang. 2003b. Predicting the physical properties of biodiesel for combustion modeling. *Trans. ASAE* 46(6): 1487-1493.

Yuan, W., A. C. Hansen, and Q. Zhang. 2004. Prediction of biodiesel fuel properties based on fatty acid composition. ASAE Paper No. 046086. St. Joseph, Mich.: ASAE.